

Network Films Composed of Conducting Polymer-Linked and Polyoxometalate-Stabilized Platinum Nanoparticles

Pawel J. Kulesza,* Malgorzata Chojak, Katarzyna Karnicka,
Krzysztof Miecznikowski, Barbara Palys, and Adam Lewera

Department of Chemistry, University of Warsaw, Pasteura 1, PL-02-093 Warsaw, Poland

Andrzej Wieckowski

Department of Chemistry, Roger Adams Laboratory, University of Illinois,
Urbana, Illinois 61801

Received January 22, 2004. Revised Manuscript Received July 12, 2004

The ability of Keggin-type phosphododecamolybdates ($\text{PMo}_{12}\text{O}_{40}^{3-}$) to undergo chemisorption and to form anionic monolayers on platinum surfaces is explored here to produce stable colloidal solutions of polyoxometalate-protected platinum nanoparticles (size, 5–10 nm, as determined by transmission electron microscopy and scanning tunneling microscopy). By dip-coating in the above solution, the particles can readily be assembled on carbon electrode substrates. The layer-by-layer method, which involves alternate exposures to the solutions of $\text{PMo}_{12}\text{O}_{40}^{3-}$ -stabilized Pt nanoparticles and anilinium cations, has been utilized to grow in a controlled manner hybrid network films in which the negatively charged layers of polyoxometalate-protected Pt nanoparticles are linked, or electrostatically attracted, by ultrathin positively charged polyaniline layers. The phosphomolybdate-decorated Pt nanoparticles (immobilized within ultrathin polyaniline film) are attractive for electrocatalysis: they show promising reactivity toward the electroreduction of oxygen.

Introduction

A great deal of recent research has been centered around the development of nanosized assemblies at solid surfaces that can produce functionalized interfaces with well-defined composition, structure, reactivity, and thickness.¹ In this context, a substantial impetus is given to the investigation of nanometer scale metal particles with respect to both to their fundamental importance and to possible applications in many areas, including molecular and nanoscale electronic and optical devices,^{1,2} sensors,³ and catalysis and electrocatalysis.^{4–7} Fabrication, assembly, alignment, interconnection, electronic properties, and reactivity of such nanosized materials are crucial facets of this growing field.^{8–10} Nanoparticles are typically characterized by small aver-

age size diameter, narrow size distribution, and similar shapes, and they often feature alkyl stabilizing agents.¹¹ For example, dense robust monolayers of alkanethiolates are capable of passivating gold nanoparticles to produce alkanethiolate-monolayer-protected clusters or nanoparticles of gold.^{8–13} An important function of alkanethiolates is to separate the metal (Au) particles in order to reduce their agglomeration, an effect that leads to their degradation. Single electron events (so-called Coulomb staircase charging) have been observed in the network films of gold nanoparticles stabilized and functionalized with thiol ligands.^{8–15} The use of nanometer-sized metal particles (e.g. gold and silver) for building high-order arrays with specific electronic functions can be envisioned.¹⁴

Nanoparticles of metals from the platinum group, in particular Pt and its alloys, are interesting electrocatalytic materials that are characterized by high surface area to volume ratios and exhibit promising reactivity toward systems of importance to fuel cell technology, including the reduction of oxygen and the oxidation of hydrogen or methanol. Recently, the feasibility of preparation of alkanethiol-protected Pt,¹⁶ Au/Pt alloy,¹⁷

* To whom correspondence should be addressed. Fax: +48-22-8225996. E-mail address: pkulesza@chem.uw.edu.pl.

(1) Fendler, J. H., Ed. *Nanoparticles and Nanostructured Films*; Wiley-VCH: Weinheim, Germany, 1998.

(2) Credo, G. M.; Boal, A. K.; Das, K.; Galow, T. H.; Rotello, V. M.; Feldheim, D. L.; Gorman, C. B. *J. Am. Chem. Soc.* **2002**, *124*, 9036.

(3) Mirkin, C. A. *Inorg. Chem.* **2000**, *39*, 2258.

(4) Carrette, L.; Friedrich, K. A.; Stimming, U. *Chem. Phys. Chem.* **2000**, *1*, 162.

(5) Park, S.; Yang, P.; Corredor, P.; Weaver, M. J. *J. Am. Chem. Soc.* **2002**, *124*, 2428.

(6) Waszczuk, P.; Solla-Gullon, J.; Kim, H.-S.; Tong, Y. Y.; Montiel, V.; Aldaz, A.; Wieckowski, A. *J. Catal.* **2001**, *203*, 1.

(7) Reetz, M. T.; Lopez, M.; Grunert, W.; Vogel, W.; Mahlendorf, F. *J. Phys. Chem. B* **2003**, *107*, 7414.

(8) Templeton, A. C.; Wuelfing, W. P.; Murray, R. W. *Acc. Chem. Res.* **2000**, *33*, 27.

(9) Brust, M.; Walker, M.; Bethell, D.; Schiffrin, D. J.; Whyman, R. *J. Chem. Soc. Chem. Commun.* **1994**, 801.

(10) Horswell, S. L.; O'Neil, I. A.; Schiffrin, D. J. *J. Phys. Chem. B* **2001**, *105*, 941.

(11) Petroski, J. M.; Green, T. C.; El-Sayed, M. A. *J. Phys. Chem. A* **2001**, *105*, 5542.

(12) Zamborini, F. P.; Leopold, M. C.; Hicks, J. F.; Kulesza, P. J.; Malik, M. A.; Murray, R. W. *J. Am. Chem. Soc.* **2002**, *124*, 8958.

(13) Bethell, D.; Brust, M.; Schiffrin, D. J.; Kiely, C. *J. Electroanal. Chem.* **1996**, *409*, 137.

(14) McConnell, W. P.; Novak, J. P.; Brousseau, L. C.; Fuierer, R. R.; Tenent, R. C.; Feldheim, D. L. *J. Phys. Chem. B* **2000**, *104*, 8925.

(15) Shiang, J. J.; Heath, J. R.; Colier, C. P.; Saykally, R. J. *J. Phys. Chem. B* **1998**, *102*, 3425.

or alkyl isocyanide-derived¹⁸ and mercaptoaniline-functionalized¹⁹ platinum nanoparticles has been described, but so far, their utility for the electrocatalysis of fuels has not been clearly demonstrated. On the other hand, immobilization of the colloidal platinum nanoparticles within mixed metal oxide nanostructures has been considered for the preparation of effective electrocatalysts for the oxidation of fuels.²⁰ Moreover, it has been established that dispersion, size, and morphology of metal particles is further improved by the addition of polymers.^{21,22} When it comes to the preparation of nanosized metal colloids, the presence of such stabilizers as polymers, surfactants, or special ligands prevents formation of insoluble bulk metal particles.

Polyoxometalates are known to form self-assembled monolayers on common solid electrode substrates.^{23–27} Keggin-type heteropolyanions of molybdenum and tungsten are particularly attractive because of their ability to adsorb irreversibly on carbon and metal surfaces to form structured films. In the present work, we explore this phenomenon to stabilize platinum nanoparticles, and we develop an approach that can be viewed as an inorganic alternative to the well-known concept of fabrication of monolayer-protected clusters of gold by strong chemisorption of organic alkanethiolates.^{8–10} We demonstrate that commercially available platinum clusters can be dispersed in polyoxometalate (e.g. dodecamolybdophosphate) solutions to form stable sols consisting of Pt nanoparticles of ca. 5–10 nm diameter. In view of the previous reports^{23,24,26,27} describing self-assembly of phosphomolybdate on solid surfaces, it is reasonable to expect that it forms negatively charged monolayers on platinum nanoparticles. Therefore, polyoxometalate should stabilize particles (and prevent their agglomeration) not only due to its physical presence but also electrostatically, thanks to the existence the repulsion forces. We can link polyoxometalate-stabilized (protected) platinum nanoparticles by creating ultrathin polymer (polyaniline) bridges to form network hybrid films on glassy carbon. Polyaniline has been chosen as a model electroactive polymer stable in acid media. The whole concept is based on multiple formations of two-dimensional arrays and three-dimensional networks composed alternately of ultrathin^{27,28} conducting polymer (e.g. polyaniline) layers and dodecamolybdophosphate-protected platinum nanoparticles. Since it is well-

known that reactivity and catalytic characteristics of metal particles are affected by specific electronic properties of supporting inorganic oxides,²⁰ we address briefly the system's ability to electrocatalyze reduction of oxygen.

Experimental Section

Phosphododecamolybdic acid, $\text{H}_3\text{PMo}_{12}\text{O}_{40}$ (PMo_{12}), and aniline monomer were obtained from Fluka. Platinum black clusters (surface area, $20 \text{ m}^2 \text{ g}^{-1}$) were obtained from Johnson&Matthew. All other chemicals were reagent grade purity, and they were used as received. Solutions were prepared using doubly distilled and subsequently deionized (Millipore Milli-Q) water. Ultrahigh purity argon gas was used to deaerate investigated solutions. Experiments were carried out at room temperature ($20 \pm 2^\circ \text{C}$).

Electrochemical measurements were done with CH Instruments (Austin, TX) Model 750 and Bioanalytical Systems (West Lafayette, IN) BAS Model 100BW workstations. A standard three-electrode cell was used. A platinum disk (diameter, 4 mm) from Mineral, Poland, or a glassy carbon disk (diameter, 3 mm) from BAS, served as a working electrode. The counter electrode was made from Pt wire. All potentials were expressed versus the saturated (KCl) Ag/AgCl electrode.

Before modification, a platinum electrode substrate was activated by potential cycling from -0.2 to 1.4 V in $0.5 \text{ mol dm}^{-3} \text{ H}_2\text{SO}_4$ for 1–2 h, whereas a glassy carbon substrate was subjected to polishing (on a cloth) with successively finer grade aqueous alumina slurries (grain size, $5\text{--}0.5 \mu\text{m}$). The Pt surface was modified with ultrathin PMo_{12} adsorbate by dipping it for 30 min in an aqueous solution of $2 \text{ mmol dm}^{-3} \text{ H}_3\text{PMo}_{12}\text{O}_{40}$.

To produce polyoxometalate-protected platinum nanoparticles, a suspension of a known amount (0.33 g) of Pt black was formed in 5 mmol dm^{-3} aqueous PMo_{12} solution (10 cm^3). The suspension was sonicated for 2 h and left overnight. Then, it was centrifuged, and the supernatant solution was removed and replaced with a fresh PMo_{12} solution. The centrifuging procedure was typically repeated three or four times until the final PMo_{12} suspension of Pt nanoparticles was permanently yellow. Any yellow discoloring and the appearance of the green-blue color would imply the existence of chemical interaction involving interfacial oxidation of Pt by PMo_{12} , presumably followed by its chemisorption and the simultaneous partial reduction to heteropolyblue. Later, the PMo_{12} solution was decanted, and the centrifuging procedure was repeated three times with water. The resulting Pt- PMo_{12} colloidal solution was stable for at least 1 month.

The network films were assembled through the alternate immersion scheme in a manner analogous to the procedure described previously²⁷ for the fabrication of robust three-dimensional multilayer hybrid assemblies of PMo_{12} and ultrathin polyaniline layers. The main difference concerns the fact that, instead of a simple PMo_{12} solution, the PMo_{12} colloidal suspension of Pt nanoparticles was used. The glassy carbon electrode was serially exposed to Pt- PMo_{12} solution, each time for 30 min, and rinsed with water. Between the steps, the electrode was exposed to a 0.07 mol dm^{-3} solution of aniline in $0.5 \text{ M H}_2\text{SO}_4$ for 10 min followed by electrochemical polymerization by potential cycling (at 50 mV s^{-1}) from -0.1 to 0.85 V in $0.5 \text{ mol dm}^{-3} \text{ H}_2\text{SO}_4$ and thorough rinsing with water. Formation of ultrathin films of polyaniline (PANI) occurred during positive potential cycles where anilinium monomers (electrostatically attracted within negatively charged PMo_{12}) were oxidized to dications and, subsequently, electropolymerized.²⁷ By repeated and alternate treatments in the appropriate solutions, the amount of material on the electrode surface can be increased in a systematic manner²⁷ up to at least 10 "bilayers" of PMo_{12} -stabilized Pt and PANI.

Transmission electron microscopy (TEM) images were obtained using a JEOL 2010F microscope (and the voltage of 200 kV was applied). The samples were prepared by placing (with

(16) Sarathy, K. V.; Raina, G.; Yadav, R. T.; Kulkarni, G. U.; Rao, C. N. R. *J. Phys. Chem. B* **1997**, *101*, 9876.

(17) Hostetler, M. J.; Zhong, C. J.; Yen, B. K. H.; Andereg, J.; Gross, S. M.; Evans, N. D.; Porter, M.; Murray, R. W. *J. Am. Chem. Soc.* **1998**, *120*, 9396.

(18) Horswell, S. L.; Kiely, C. J.; O'Neil, I. A.; Schiffrin, D. J. *J. Am. Chem. Soc.* **1999**, *121*, 5573.

(19) Perez, H.; de Souza, R. M. L.; Pradeau, J. P.; Albouy, P.-A. *Chem. Mater.* **2001**, *13*, 1512.

(20) Reetz, M. T.; Lopes, M.; Grunert, W.; Vogel, W.; Mahlendorf, F. *J. Phys. Chem. B* **2003**, *107*, 7414.

(21) Miyazaki, A.; Nakano, Y. *Langmuir* **2000**, *16*, 7109.

(22) Ahmadi, T. S.; Wang, Z. L.; Green, T. C.; Henglein, A.; El-Sayed, M. A. *Science* **1996**, *272*, 1924.

(23) Ingersoll, D.; Kulesza, P. J.; Faulkner, L. R. *J. Electrochem. Soc.* **1994**, *141*, 140.

(24) Kuhn, A.; Anson, F. C. *Langmuir* **1996**, *12*, 5481.

(25) Ge, M.; Zhong, B.; Klemperer, W.; Gewirth, A. A. *J. Am. Chem. Soc.* **1996**, *118*, 5812.

(26) Kuhn, A.; Mano, N.; Vidal, C. *J. Electroanal. Chem.* **1999**, *462*, 187.

(27) Kulesza, P. J.; Chojak, M.; Miecznikowski, K.; Lewera, A.; Malik, M. A.; Kuhn, A. *Electrochem. Commun.* **2002**, *4*, 510.

(28) Turyan, I.; Mandler, D. *J. Am. Chem. Soc.* **1998**, *120*, 10733.

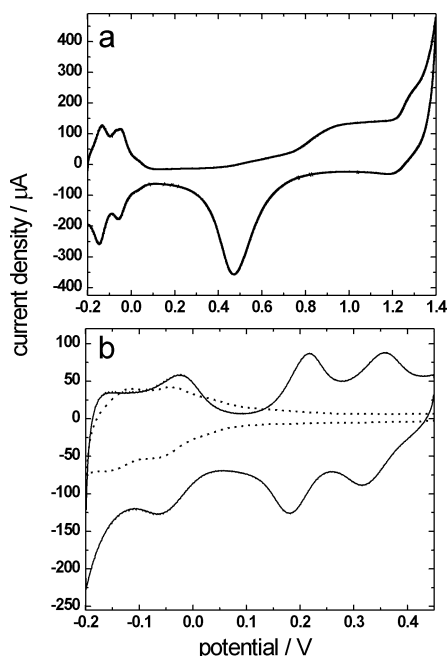


Figure 1. Cyclic voltammetric responses of (a) bare platinum electrodes and (b) platinum electrodes modified with a PMo_{12} monolayer. Electrolyte, $0.5 \text{ mol dm}^{-3} \text{ H}_2\text{SO}_4$ (saturated with argon); scan rate, 50 mV s^{-1} ; geometric surface area, 0.125 cm^2 . Dotted line shows the response of bare Pt.

microsyringe) a drop of Pt- PMo_{12} colloidal solution (prepared as described above but diluted 100 times) onto a carbon-coated copper mesh grid. Consequently, the dry specimen consisting of Pt nanoparticles embedded into the carbon film was obtained. The grid was mounted into a single-tilt TEM holder and used for analysis. The particle size analysis was achieved with the Gatan Digital Micrograph software. The samples were also subjected to energy dispersive elemental analysis by X-ray (EDX) unit coupled with JEOL Model JSM-5400 scanning electron microscope.

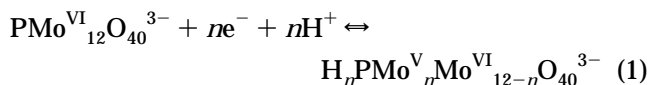
Scanning tunneling microscopy (STM) images were obtained ex-situ (in air) using EasyScan Nanosurf AG (Switzerland) instrument. The tips of Pt/Ir (90/10) wires of 0.25 mm diameter were formed mechanically, and they were used as probes. The scanning was achieved in the constant-current mode at positive sample bias of $50\text{--}100 \text{ mV}$ and tunneling current of $1\text{--}2 \text{ nA}$.

Infrared spectra were measured with Shimadzu 8400 FTIR spectrometer. The Infrared reflectance absorption spectra (IRRAS) were recorded using a Specular Reflectance Accessory Model 500 produced by Spectra Tech. The beam incidence angle was equal to 80° with respect to the surface normal. Typically 500 scans were averaged for a single reflectance spectrum.

Results and Discussion

Cyclic voltammetric responses of (a) bare platinum disk electrodes and (b) platinum disk electrodes subsequently modified with a monolayer of PMo_{12} are illustrated in Figure 1. The data of Figure 1a, particularly the characteristic hydrogen adsorption and Pt/PtO peaks, are consistent with the existence of a clean (activated) platinum surface.²⁹ By analogy to the voltammetric behavior of the PMo_{12} monolayer^{27,30–33}

or the PMo_{12} -PANI composite film^{34–36} deposited on glassy carbon or gold, the three sets of peaks observed in Figure 1b shall be attributed to three consecutively appearing, approximately two-electron redox reactions:



where the total number of electrons involved (n) is expected to be equal to 6. It is apparent, from the comparison of curves a and b (Figure 1), that while the third most negative set of PMo_{12} voltammetric peaks appears in the potential range where hydrogen adsorption peaks would appear on bare clean Pt, the PMo_{12} -stabilized Pt nanoparticles retain their electrocatalytic properties toward the proton discharge (hydrogen evolution). The detailed study about chemisorption of PMo_{12} and its behavior on Pt and other solid substrates will be the subject of a separate work.

From the cyclic voltammogram of a clean platinum electrode (Figure 1a), namely from the charge under the hydrogen reduction peaks,²⁹ one can determine the true surface area of the platinum substrate. Consequently, by comparison to the charge under the cathodic peak of the second PMo_{12} redox process that displays the most clearly defined response (at about 0.2 V in Figure 1b), a “true” surface coverage of PMo_{12} equal to $3 \times 10^{-10} \text{ mol cm}^{-2}$ can be found. The latter value translates into ca. $18 \times 10^{13} \text{ PMo}_{12}$ units per cm^2 . For comparison, assuming the ideal cubic symmetry and the PMo_{12} unit cell parameter of 1.1 nm , close geometric packing of PMo_{12} units within a monolayer on the surface, and using the Avogadro’s number, we obtain the loading of $8 \times 10^{13} \text{ PMo}_{12}$ units per cm^2 . Thus, the surface concentration equal to $3 \times 10^{-10} \text{ mol cm}^{-2}$ is consistent with the coverage of PMo_{12} (on Pt) comparable to, or somewhat exceeding, the monolayer level.

It is reasonable to expect that PMo_{12} undergoes similar adsorption at the monolayer level on nanosized Pt (platinum black). The procedure of stabilizing of Pt nanoparticles and protecting them from agglomeration by modification with monolayers of PMo_{12} anions involves a few exposures of the Pt clusters (built from the agglomerated Pt nanoparticles) to PMo_{12} solutions and consecutive centrifuging aiming at the formation of a colloidal suspension of nanosized platinum in water (as described in the Experimental Section). The existence of electrostatic repulsive interactions between the negatively charged PMo_{12} monolayers on the Pt surfaces is likely to be responsible for the splitting of Pt clusters to parent nanoparticles.

Figure 2 illustrates a representative TEM image of Pt nanoparticles that have been synthesized in the presence of PMo_{12} anions and embedded into the carbon film. The image shows that the nanoparticles generally have a dark (electron dense) central core (originating

(29) Conway, B. E.; Kozłowska, H. A.; Sharp, W. B. A.; Criddle, E. *Anal. Chem.* **1973**, *45*, 1331.

(30) Cheng, L.; Niu, L.; Gong, J.; Dong, S. *Chem. Mater.* **1999**, *11*, 1465.

(31) Cheng, L.; Pacey, G. E.; Cox, J. A. *Electrochim. Acta* **2001**, *46*, 4223.

(32) Martel, D.; Kuhn, A.; Kulesza, P. J.; Galkowski, M. T.; Malik, M. A. *Electrochim. Acta* **2001**, *46*, 4197.

(33) Sine, G.; Hui, C. C.; Kuhn, A.; Kulesza, P. J.; Miecznikowski, K.; Chojak, M.; Paderewska, A.; Lewera, A. *J. Electrochem. Soc.* **2003**, *150*, C351.

(34) Lira-Cantu, M.; Gomez-Romero, P. *Chem. Mater.* **1998**, *10*, 698.

(35) Bidan, G.; Genies, E. M.; Lapkowski, M. *J. Chem. Soc., Chem. Commun.* **1988**, *5*, 533.

(36) Bidan, G.; Lapkowski, M.; Travers, J. P. *Synth. Met.* **1989**, *28*, C113.

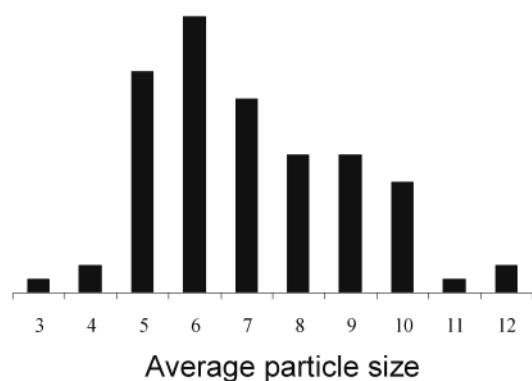
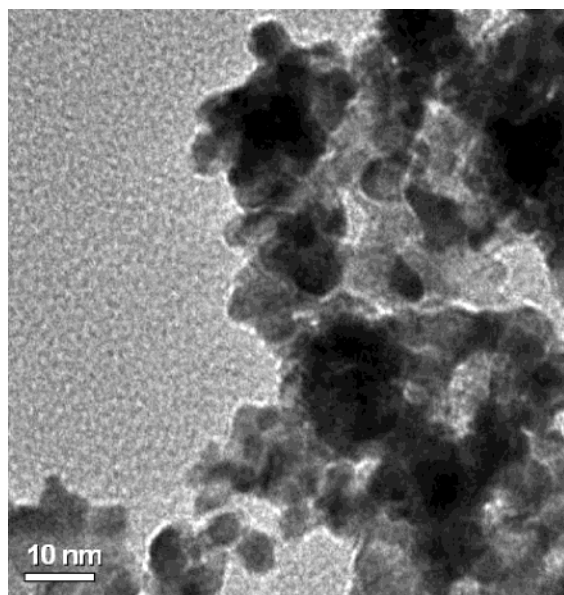


Figure 2. Transmission electron micrograph (TEM) of the PMo_{12} -stabilized platinum nanoparticles.

from Pt), and they are surrounded by a lighter shell (originating from the polyoxometalate outer layer and carbon matrix) that hinders somewhat determination of size distribution. Judging from the particle size dispersion (histogram), most of particles have diameters ranging from 5 to 10 nm. Neither dilution nor extensive sonication of the original suspension has led to any significant changes in the nanoparticle size distribution. Their average size (obtained over many images by measuring at least 30–50 particles each time) is 6.85 nm. Ideally, if Pt nanoparticles were densely and completely covered with PMo_{12} (unit cell parameter, ca. 1.1 nm) monolayers, one would expect the sizes of the Pt cores to be roughly 4.6–4.7 nm.

Figure 3 shows a cyclic voltammetric response (recorded in argon-saturated $0.5 \text{ mol dm}^{-3} \text{ H}_2\text{SO}_4$) of a glassy carbon electrode modified with an ultrathin film of platinum nanoparticles derivatized with PMo_{12} . The spontaneous deposition of such Pt particles on glassy carbon was achieved by simple dipping of the electrode substrate in the PMo_{12} -stabilized suspension. Attachment of Pt nanoparticles was presumably facilitated by the presence of “bridging” polyoxometalate (PMo_{12}) molecules capable of chemisorbing on both platinum and glassy carbon.²⁷ It is noteworthy that the voltammetric pattern of Figure 3 exhibits both the peaks characteristic of PMo_{12} (in the potential range from 0.1 to 0.45

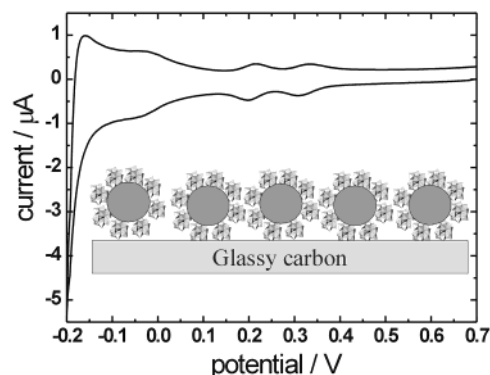


Figure 3. Cyclic voltammetric response of an ultrathin film of PMo_{12} -protected Pt nanoparticles self-assembled on glassy carbon. Geometric surface area, 0.07 cm^2 . Other conditions were the same as for Figure 1.

V) and the typical hydrogen evolution/proton discharge currents (originating from the presence of catalytic Pt) at potentials more negative than -0.1 V . The latter result, when confronted with the response of bare bulk Pt electrode (Figure 1a) or the behavior of naked Pt nanoparticles,⁶ indicates qualitatively that the electrocatalytic properties of Pt toward the reduction of protons are retained, if not enhanced, upon interfacial derivatization with of PMo_{12} .

EDX analysis of polyoxometalate-stabilized nanoparticles (immobilized on glassy carbon) implies the presence of both Mo and Pt as major elemental components. Despite use of the EDX acquisition software to quantify elements on the surface, the analytical results are only semiquantitative. Nevertheless, the relative molar ratio of Mo to Pt does not exceed 1:10. Further, assuming that all polyoxometalate-stabilized Pt nanoparticles are spherical, their average diameter is 6.9 nm (which corresponds to a content of nearly 11 000 Pt atoms), and their surfaces are completely covered with ideal monolayers of closely packed cubic (12 Mo atoms containing) phosphomolybdates of ca. 1.1 nm unit cell parameter, one can estimate the molybdenum mole percentage (assuming that $\% \text{ Mo} + \% \text{ Pt} = 100\%$) to be larger than 5%. The above results are consistent with the hypothesis that the coverage of our Pt nanoparticles with PMo_{12} is on the level of a monolayer.

The presence of chemisorbed PMo_{12} on platinum was also evident from the ex situ FTIR examination of the surface of gold-covered glass onto which the PMo_{12} -stabilized Pt nanoparticles were self-assembled (Figure 4b). The latter spectrum was analogous to that characteristic of PMo_{12} in KBr (Figure 4a). The fact that P–O–Mo stretching mode^{34,37,38} appearing at 1078 cm^{-1} in Figure 4b does not differ significantly from that typical for bulk PMo_{12} (1064 cm^{-1} in Figure 4a) implies that inner P–O bonds are not substantially affected by chemisorption of PMo_{12} on Pt. Some increase in the frequencies of oxygen-bridged Mo–O–Mo stretching modes from 787 and 870 cm^{-1} (Figure 4a) to 821 and 884 cm^{-1} (Figure 4b), respectively, may originate from “strengthening” of the polyanion structure and the

(37) Fournier, M.; Rocchiccioli-Deltchev, C.; Kazansky, L. P. *Chem. Phys. Lett.* **1994**, 223, 297.

(38) Hasik, M.; Pron, A.; Pozniczek, J.; Bielanski, A.; Piwowarska, Z.; Kruczala, K.; Dziembaj, R. *J. Chem. Soc., Faraday Trans.* **1994**, 90, 2099.

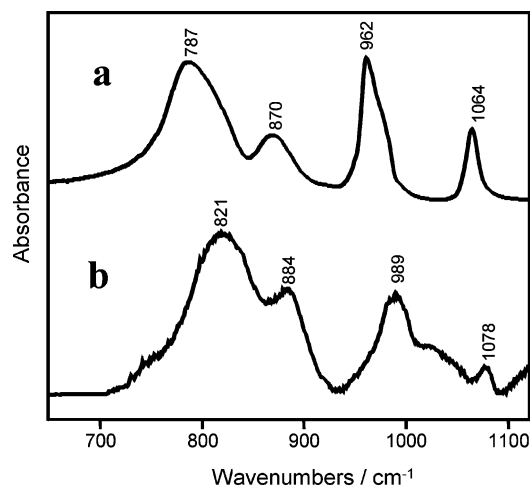


Figure 4. FTIR spectra of (a) phosphododecamolybdic acid in KBr and (b) PMo_{12} -protected Pt nanoparticles self-assembled on a gold-coated glass slide.

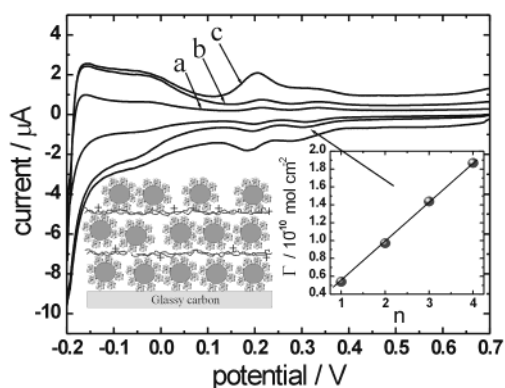


Figure 5. Cyclic voltammograms recorded at 50 mV s^{-1} (in argon-saturated $0.5 \text{ mol dm}^{-3} \text{ H}_2\text{SO}_4$) following application of (a) one, (b) two, and (c) four cycles of alternate treatments in the colloidal solution of PMo_{12} -protected Pt and the solution of anilinium ions. Insets illustrate (left) the attachment of PMo_{12} -protected Pt particles via ultrathin PANI bridges and (right) the dependence of the loading of PMo_{12} (chemisorbed on Pt nanoparticles) on a number of the alternate immersion cycles. Geometric surface area of glassy carbon substrate, 0.07 cm^2 .

related decrease of distance between the anions upon formation of a compact PMo_{12} monolayer on Pt. The shift of external (terminal) $\text{Mo}=\text{O}$ bond frequency from 962 cm^{-1} (Figure 4a) to 989 cm^{-1} (Figure 4b) is presumably due to interactions between the Pt substrate and the adsorbed PMo_{12} .

It has been previously demonstrated²⁷ that alternate immersions ("dipping cycles") in heteropolyanion (PMo_{12}) and monomer (aniline) solutions leads to the formation of organized hybrid inorganic (polyoxometalate)–organic (conducting polymer) multilayer films. In the present work, we show that the PMo_{12} -protected (stabilized) Pt nanoparticles can be linked together by polyaniline (PANI) bridges to form a network film, as illustrated in the left inset to Figure 5. We started here from the formation of an initial ultrathin layer of PMo_{12} -stabilized Pt nanoparticles on glassy carbon substrate. Figure 6a shows the STM image corresponding to the spontaneous deposition of PMo_{12} -covered Pt nanoparticles on glassy carbon. The uniformly and densely dispersed light spots shall be attributed to the nanostructured platinum. In the next step (Figure 5), the

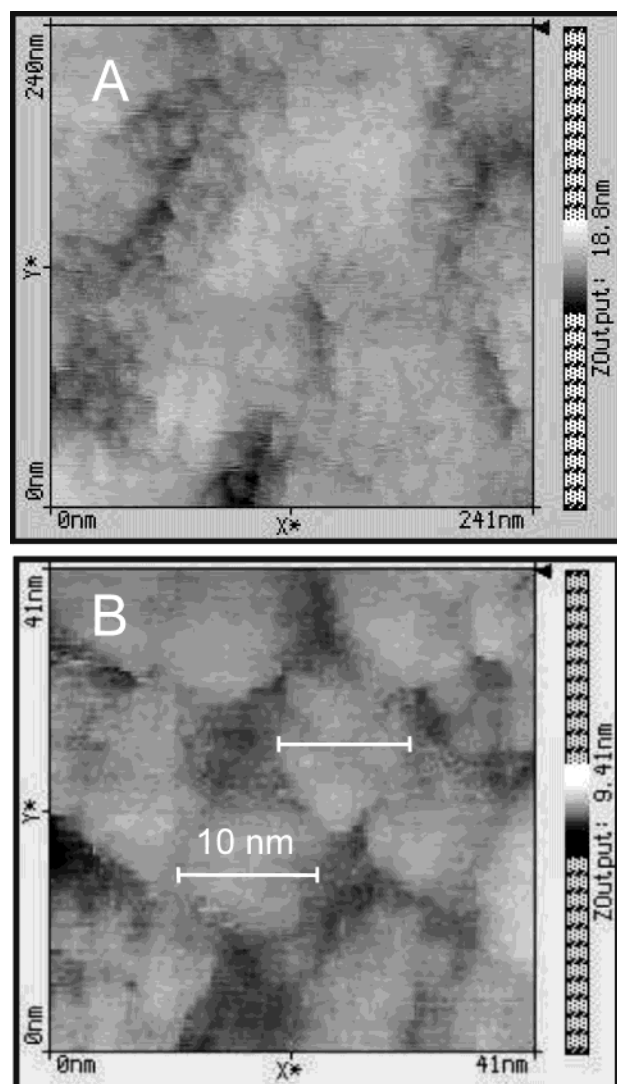


Figure 6. STM images of PMo_{12} -protected Pt nanoparticles self-assembled on (a) bare glassy carbon (as for Figure 3) and (b) PMo_{12} –PANI bilayer (see inset to Figure 7).

Pt– PMo_{12} modified electrode was exposed to the anilinium monomer solution for 10 min, then it was removed, rinsed, dried, and subjected to three voltammetric cycles in $0.5 \text{ mol dm}^{-3} \text{ H}_2\text{SO}_4$ in the potential range up to 0.85 V . The latter procedure resulted in the complete polymerization of anilinium ions and formation of an ultrathin polyaniline (PANI) film.²⁷ The result is consistent with the view that PMo_{12} chemisorbed on Pt particles is not only stable but also retains its negative charge necessary for electrostatic attraction of positively charged ultrathin PANI layers. Each additional voltammogram in Figure 5 corresponds to the film response related to the formation of an extra Pt– PMo_{12} /PANI bilayer. In other words, the successful formation of the multilayer network film consisting of Pt– PMo_{12} and PANI is demonstrated by the increase of voltammetric peak currents (Figure 5) following alternate treatments in Pt– PMo_{12} colloidal suspension and the anilinium solution (the latter step was as a rule combined with the interfacial electropolymerization of PANI as described above). Characteristic infrared peaks³⁴ of both PMo_{12} and PANI have been found in the FTIR spectrum (recorded as for Figure 4b) of the multilayer PANI-linked PMo_{12} -stabilized Pt network film. The uniform

distribution of Pt-PMo₁₂ and PANI layers is apparent from the monotonic increase of the PMo₁₂ voltammetric peaks during alternate immersion cycles (Figure 5). By plotting the film loading (calculated from the charge under the most positive PMo₁₂ reduction peak), a linear dependence versus a number of treatments in Pt-PMo₁₂ solutions (slope 0.5×10^{-10} mol cm⁻² per immersion cycle) has been obtained (see right inset to Figure 5). Judging from the increase of currents related to the hydrogen evolution at potentials more negative than -0.15 V (Figure 5), the loading of platinum is systematically increased during the film growth through the alternate immersion scheme.

The most positive set of peaks appearing in the multilayer film at about 0.3 V (Figure 5) shall be attributed, as in the case of a PMo₁₂ monolayer (Figure 1b), to the first (most positive) two-electron redox reaction of PMo₁₂. The fact that the second set of PMo₁₂ peaks at about 0.18 V is larger than that at ca. 0.3 V (Figure 5) originates from the overlapping of the second two-electron reduction of PMo₁₂ with the PANI reaction, namely the reduction of emeraldine to leucoemeraldine.²⁷ It is reasonable to expect that, due to the good charge-distributing capabilities of Pt-PMo₁₂ nanostructures, the redox behavior of ultrathin PANI interlayers (bridges) is more redox facile in comparison to the typical behavior of a conventional PANI film.^{27,36} On the other hand, the fact that the polyoxometalate response persists for several layers indicates significant long-range conductivity within the system. Certainly, the fast dynamics of charge transport in our composite system is facilitated not only by high self-exchange rate between PMo₁₂ redox centers and the presence of dispersed Pt particles but also by the fact that the two most positive redox processes of PMo₁₂ lie in the potential range where PANI is conductive. When the PMo₁₂ voltammetric peak currents characteristic of the multilayer film (at ca. 0.2 and 0.3 V in Figure 5) were plotted versus scan rate, the dependencies were practically linear (effectively with zero intercept) up to ca. 5 V s⁻¹. Such behavior is consistent with the surface type behavior of the system as well as with the fast dynamics of charge transport in the vertical dimension, i.e., perpendicular to the electrode surface.

Since an ultimate goal of our research is to produce Pt nanostructures exhibiting promising electrocatalytic properties, we have examined reactivity of PMo₁₂-stabilized platinum nanoparticles toward reduction of dioxygen in 0.5 mol dm⁻³ H₂SO₄ (Figure 7). The Pt-PMo₁₂ nanocenters were dispersed within the ultrathin PANI film that was self-assembled on glassy carbon substrate as described earlier.²⁷ As illustrated in the inset to Figure 7, PMo₁₂-protected Pt nanoparticles were introduced (or electrostatically attracted) to the bilayer film formed from the PMo₁₂ monolayer chemisorbed on glassy carbon (inner layer) and the ultrathin layer of positively charged PANI (outer layer). Figure 6b shows the STM image of such a film containing nanostructured platinum. Careful examination of the STM data implies that the size of platinum particles is ca. 6–10 nm. Even at a small loading of platinum, the system was well-behaved and the voltammetric peak for the reduction of oxygen at PMo₁₂-protected Pt appeared at 0.51 V (Figure 7). This peak potential value is comparable to

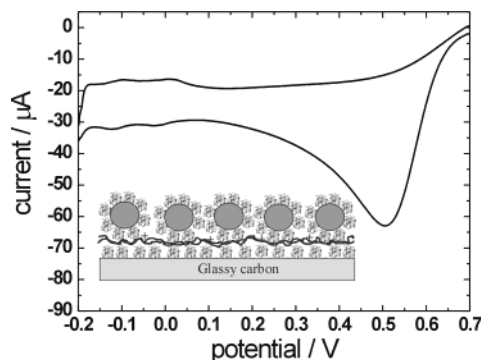


Figure 7. Electrocatalytic reduction of oxygen at the bilayer film of PMo₁₂/PANI (on glassy carbon) into which PMo₁₂-protected Pt nanoparticles were immobilized (see inset). Electrolyte, 0.5 mol dm⁻³ H₂SO₄ saturated with oxygen (ca. 0.8 mmol dm⁻³);³⁹ scan rate, 50 mV s⁻¹.

those reported previously for oxygen reduction at polycrystalline Pt or platinized tungsten oxide electrode.³⁹ Our preliminary rotating ring (Pt)-disk (glassy carbon) voltammetric studies show that the oxygen reduction was a diffusion-controlled process (at least up to 4900 rpm), and no H₂O₂ was produced in the potential range from 0.3 to 0.7 V. The latter observation implies that overall process must have involved four electrons and proceeded directly to H₂O. What is even more important from the data of Figure 7 is that high reactivity of Pt nanoparticles toward the reduction of oxygen was retained in the presence of PMo₁₂ and the PANI environment. Conducting polymers have been already shown to serve as attractive matrixes for dispersed platinum nanoparticles.^{40–43} Having in mind the chemical analogies between polyoxometalates and parent metal oxides, PMo₁₂ is expected to provide similar environment to tungsten oxides.³⁹

Conclusions

We demonstrate the possibility of stabilization of platinum nanoparticles of the size 5–10 nm by protecting them through chemisorption of polyoxometalate (PMo₁₂) monolayers on their surfaces. Since PMo₁₂-covered particles are negatively charged, they form stable colloidal solutions. The particles can be assembled together to form layers on electrode surfaces (glassy carbon). The PMo₁₂-protected Pt nanoparticles can be linked via ultrathin polymer (PANI) layers (bridges); consequently, the controlled layer-by-layer growth of polymer/nanoparticle hybrid films is feasible. The concept of alignment, interconnection, and stabilization (physical separation) of metal nanoparticles by covering them with inorganic polyoxometalates resembles somewhat the formation of colloid films of gold nanoclusters protected with organic alkanethiolates.^{8–14,16,17} But the charge propagation mechanism in our network films of PMo₁₂-stabilized nanoparticles is different from that occurring in more traditional systems of alkanethiolate-

(39) Kulesza, P. J.; Grzybowski, B.; Malik, M. A.; Galkowski, M. T. *J. Electrochem. Soc.* **1997**, *144*, 1911.

(40) Coutanceau, C.; Croissant, M. J.; Napporn, T.; Lamy, C. *Electrochim. Acta* **2000**, *46*, 579.

(41) Liu, S. Q.; Tang, Z. Y.; Wang, E. K.; Dong, S. J. *Electrochem. Comm.* **2000**, *2*, 800.

(42) Hepel, M. *J. Electrochem. Soc.* **1998**, *145*, 124.

(43) Qi, Z. G.; Pickup, P. G. *Chem. Commun.* **1998**, 15.

protected gold nanostructures. The inorganic monolayer provides metal oxide reactive centers and acts as mixed-valence, electronically conducting, and protonically conducting adsorbate. Unless derivatized, the alkanothiolate layer is insulating (dielectric), and electronic conductivity proceeds through a tunneling mechanism.¹²

The approach described here permits not only assembling conducting polymers and metal nanoparticles into network composite structures but also producing organized multilayer assemblies with specific electrocatalytic properties. Thus, physicochemical properties of polymers and reactivity of polyoxometalates and noble metal particles can be combined within network film. Our work parallels recent attempts by others showing the possibility of the layer-by-layer growth of polymer-gold nanoparticle films,⁴⁴ the synthesis of metal nanoparticles by using polyoxometalates as photocatalysts and stabilizers,⁴⁵ the application of metal (palladium)-substituted Keggin-type polyoxometalates in catalysis,⁴⁶ and fabrication of molybdate-modified Pt nanoparticles.⁴⁷ In addition to catalysis and electrocatalysis, the

modified and protected nanometer-scale metal nanoparticles are of potential utility to the assembling of electro-optical materials, devices, and sensors, including biosensors.

Acknowledgment. This work was funded by Ministry of Science (Poland) under the State Committee for Scientific Research (KBN) grants 7 T09A 05426 and 4 T09A 12225 (doctoral). K.M. acknowledges support from the University of Warsaw under BW project. M.C. appreciates fellowship from the Foundation for Polish Science (FNP). This work was also supported in part by the U.S. Department of Energy, Division of Materials Sciences under Award No. DEFG02-91ER45439, through the Frederick Seitz Materials Research Laboratory at the University of Illinois at Urbana-Champaign. The authors thank Dr. Lajos Gancs of University of Illinois for his invaluable assistance with TEM measurements. Participation in the Oxygen Reduction Network (ZSW, Ulm, Germany) is also appreciated.

CM040010P

(44) Hicks, J. F.; Seok-Shon, Y.; Murray, R. W. *Langmuir* **2002**, *18*, 2288.

(45) Troupis, A.; Hiskia, A.; Papaconstantinou, E. *Angew. Chem., Int. Ed.* **2002**, *4*, 1911.

(46) Kogan, V.; Aizenshtat, Z.; Popovitz-Brio, R.; Neumann, R. *Org. Lett.* **2002**, *4*, 3529.

(47) Flynn, N. T.; Gewirth, A. A. *Phys. Chem. Chem. Phys.* **2004**, *6*, 1310.